



ARTICLE

Color and Gloss Changes of a Lignin-Based Polyurethane Coating under Accelerated Weathering

Fatemeh Hassani Khorshidi¹, Saeed Kazemi Najafi¹, Farhood Najafi^{2,*}, Antonio Pizzi^{3,*}, Dick Sandberg⁴ and Rabi Behrooz¹

¹Department of Wood Science and Technology, Faculty of Natural Resources, Tarbiat Modares University, Tehran, Iran

²Department of Resin and Additives, Institute for Color Science and Technology, P.O. Box 16765-654, Tehran, Iran

³LERMAB, University of Lorraine, Blvd des Aiguillettes, Nancy, 54000, France

⁴Wood Science and Engineering, Luleå University of Technology, Skellefteå, Sweden

*Corresponding Authors: Farhood Najafi. Email: fnajafi@icrc.ac.ir; Antonio Pizzi. Email: antonio.pizzi@univ-lorraine.fr

Received: 17 July 2023 Accepted: 28 September 2023 Published: 11 March 2024

ABSTRACT

The purpose of this research study was to investigate the properties of polyurethane coatings based on lignin nano-particles. For this purpose, the prepared coatings were applied to pine wood surfaces and weathered artificially. Subsequently, color and gloss of the coatings were measured before and after the weathering test. Field emission scanning electron microscopy (FE-SEM) micrographs prepared from the coatings showed that the average size of nano-particles in the polyurethane substrate was approximately 500 nm. Nuclear magnetic resonance (¹³C-NMR) spectroscopy showed that strong urethane bonds were formed in the nano-lignin-based polyurethane. Differential calorimetric analysis (DSC) test revealed that the glass-transition temperature (T_g) of lignin nano-particles modified with diethylenetriamine (DETA) was 112.8°C and T_g of lignin nano-particles modified with ethylenediamine (EDA) was 102.5°C, which is lower than the T_g of un-modified lignin (114.6°C) and lignin modified with DETA (126.8°C) and lignin modified with EDA (131.3°C). The coatings modified with lignin nano-particles had a greater change in gloss. The lignin nano-particles in the modified coating are trapping hydroxyl radicals which reduces photoactivity and yellowing of the polyurethane by about 3 times compared to unmodified polyurethane coatings. After weathering test, the nano-lignin-based coating had a rougher surface with a lower contact angle (0.78°) compared to the unmodified polyurethane coating (0.85°).

KEYWORDS

Amination; propylene carbonate; lignin; biopolymer; polyurethane; coating; polyol; UN SDG 13

1 Introduction

The main purposes of coating on an exterior wooden surface are to change its appearance and to protect the wood from biological, chemical, mechanical, and physical degradation. The service life of the coating is an important factor in this context, i.e., it is desirable that the coating retains its appearance and that it does not degrade so the protective effect is lost [1–3].

One of the common bases for wood coatings is polyurethane (PU), a group of polymers that is composed of a di-isocyanate and a polyol. PUs are co-polymers that include the hard part of urethane and the soft parts



of polyester or polyether [4,5]. The hard part acts like a filler giving dimensional stability of the PU, and the soft part gives the PU its elasticity [6].

Biodegradable PUs are made from polyols, starch, fatty acids, and isocyanates [7]. Biodegradable lignin-based PUs have successfully been used in polyurethane coatings [8–10].

Problems with lignin in PUs are its low degree reaction with the other components and how it distributes itself in the polymer substrate.

The work presented here discusses the chemical modification of lignin with amine and propylene carbonate as a source of monomer in the polymerization process.

First, amine reacts additively with the double bonds of lignin and forms strong carbon and nitrogen bonds. In the next step, the modification of lignin with propylene carbonate causes the creation of reactive first-type hydroxyl groups on its five-carbon rings [11–13].

In addition to enhancing the appearance of wood, polyurethane coatings provide protection against dimensional changes, the occurrence of cracks, and degradation through destructive factors [14,15].

The purpose of the present study was to use nano-lignin compounds modified with amine and propylene carbonate for the two-step synthesis of polyol. The synthesized polyol was used as a partial replacement for common oil-based polyols in the production of PU coatings. For this purpose, the synthesized polyol resulted in a PU coating with certain and different proportions with aliphatic isocyanate N-75. In order to investigate the protective effects of the synthesized coating on wood, color and gloss were studied over time under accelerated weathering.

2 Experimental

2.1 Lignin Extraction and Modification

Sulfuric acid was added to the liquor in a mechanical pulping process proportion (20:1 mL) for precipitation and extraction of lignin. 10 grams of lignin was mixed under heating (60°C) with 3 grams of diethylenediamine (DETA), and 3 grams of ethylenediamine (EDA), 50 milliliters of methanol solution and 50 milliliters of xylene solution were added under stirring. This solution was passed through a sulfone filter. After the completion of the reaction, amino lignin was washed 4 times with methanol solution and finally dried under vacuum at (30°C). For the reaction of amino lignin with propylene carbonate, 9 grams of amino lignin was mixed with 10 grams of propylene carbonate, chloroform and dibutyltin dilaurate catalyst for 6 h at (60°C). Next, having passed through the sulfone membrane, the separated product was dried under vacuum at (30°C). All chemicals in this stage were manufactured in Germany by Merck Company.

2.2 Forming the Film and Coating the Samples

Polyurethane (PU) coating was prepared according to Table 1. The coating was applied to the surface of the pine wood surface using the film coating method with the ability to adjust the thickness of the coating to 120 micrometers. The amount of PU applied on the surfaces was $150 \pm 10 \text{ g/m}^2$, which was applied to the specimens in one step. Then the coatings were dried for one week at ambient temperature (20°C).

2.3 $^{13}\text{C-NMR}^1$ Spectroscopy

Carbon-13 nuclear magnetic resonance ($^{13}\text{C-NMR}$) spectroscopy, according to the ASTM D4273-23 standard, was used to analyze the carbon groups of lignin and nano-lignin. 400 microliters of the solvent mixture containing deuterium dimethyl sulfoxide were added to 30 mg of the lignin. This compound was transferred into $^{13}\text{C-NMR}$ tubes and the corresponding spectra were obtained by Bruker 300 MHz device

¹ Carbon-13 nuclear magnetic resonance.

made in Karlsruhe, Germany which was controlled by top spin software, with a scan value of 256 and at a temperature of (20°C). ¹³C-NMR data processing was done by MestReNova software [16].

Table 1: Lignin-based polyurethane coatings

Treatment No.	NCO- N75 (g)	AC 782 (g)	Modified lignin with -EDA-PC (%)*	Modified lignin with -DETA-PC (%)*	Modified nano-lignin with -EDA-PC (%)*	Modified nano-lignin with -DETA-PC (%)*
1	2.7	10	–	–	–	–
2	2.7	9.3	–	–	7	–
3	2.7	9.3	–	–	–	7

Note: *Based on the weight percentage of acrylic polyol AC782.

2.4 Differential Scanning Calorimetric Analysis

In the differential calorimetric analysis (DSC) method, the glass transition temperature of modified and unmodified lignin was determined by a DSC820 Mettler Toledo Calorimetry device (Mettler Toledo, Switzerland). According to the ASTM E1356-08 standard, approximately 3 mg of the lignin types were placed in a special 40-microliter aluminum container, and it was closed by a cap with a hole in the middle. An empty aluminum container was used as a reference. The samples were scanned with a flow rate of 50 ml/min in the temperature range of (25°C to 450°C) by steps of (10°C) [17].

2.5 Gel Permeation Chromatography

Two to three mg of lignin was dissolved in dimethyl sulfoxide (HPLC purity grade), Sigma-Aldrich, Chromasolve (0.1% (w/v) lithium chloride). The resulting samples were first filtered with a 0.45 µm filter before the gel permeation chromatography (GPC) test. The device (waters GPC 2000, Perkin Elmer, USA) was equipped with three columns in the form of Agilent PLgel 5 µm-10000 A, 1000 A° and 500 A° series, as well as a refractive index detector (RID) and a photodiode array detector (PDA). The mobile phase was HPLC-grade dimethyl sulfoxide containing 0.1% of lithium chloride which was used with a flow rate of 0.75 ml/min in 70 min at a column temperature of (70°C). Calibration was performed according to styrene sulfonate standards and, in the lower range, monomeric- and dimeric-model lignin. Chromatograms were prepared using a detector response in 280 nm signal. Finally, the molecular weight of average number, the molecular weight of average weight, and the dispersion index for lignin were calculated by the software based on the absorption in the specified range.

2.6 FE-SEM² Electron Microscopy

Micrographs of the cross-sections of samples from the coated specimens were taken in a field emission scanning electron microscopy (FE-SEM) (HITACHI 4160-S) model made in Japan. Next, in order to create contrast, electron signals from different points of the sample were collected through the detector of the device to form the topography related to each point of the sample on the screen.

2.7 Contact-Angle Measurement

The drop method was used before and after mixing lignin to measure the contact angle of PU films and coated specimens. This test was performed at a temperature of (23°C) and 50% relative humidity (RH). The contact angle was recorded by ImageJ software.

² Field Emission Scanning Electron Microscopes.

2.8 Surface-Roughness Measurement

The surface roughness was measured using the Surface Roughness Tester, in the direction perpendicular to the fibers through the profilometric method. A profilometer was used to measure the average surface roughness values (Ra) as an average of 10 points including 5 peaks and 5 valleys (Rz).

2.9 Accelerated Weathering Test

A QUV weatherometer moderner model made in Germany was used to expose the coated specimens to ultra-violet (UV) radiation and moisture according to the ASTM D4587-11 process [18]. In the weathering cycle, the specimens received light alone in 102 min, followed by 18 min of light and spraying. The water was added simultaneously with a radiation intensity of 41.5 W/m^2 between the wavelengths of 300 and 400 nm, and humidity was applied to a maximum of $65 \pm 5\%$ in the distances where only light was irradiated.

X-Rite Eye one SP-64 Spectrophotometer Konica Minolta FD-7.

2.10 Color Measurement

Colour measurements (L^* , a^* and b^* spatial parameters, where L^* indicates lightness, and a^* and b^* are respectively red/green and blue/yellow parameters, respectively) were undertaken using a CIELAB colorimeter X-Rite Eye one SP-64 Spectrophotometer, v2.11 Build EB05 Version, made in UK. The colour was measured on the coated wood specimens after watering. The colour difference ΔE between two different colours can be calculated as the distance between two points in this CIELAB-space, according to Eq. (1):

$$\Delta E^* = \sqrt{(\Delta E^*)^2 + (\Delta a^*)^2 + (\Delta b^*)^2} \quad (1)$$

2.11 Gloss Measurement

According to Fig. 1, to check the quality of the polyurethane coating surface, the specular gloss of the coated surfaces was measured with the help of the device Rhopoint Instruments, manufactured by Novo-Gloss I.Q. Gunyo model, UK, with the geometry of 20° , 60° and 85° at a temperature of 23°C and 30% RH (Fig. 1). The glossiness of the coated surfaces was measured as presented in Tables 2 and 3.

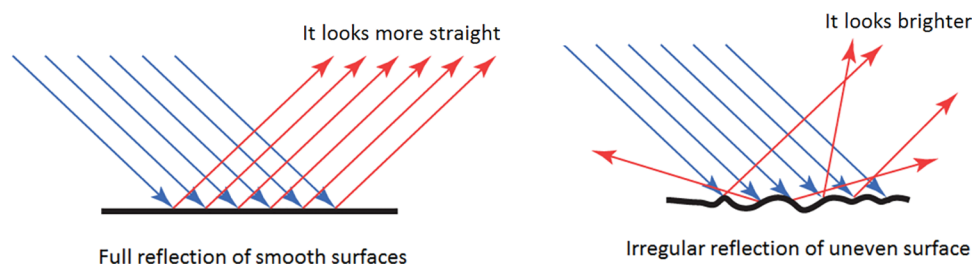


Figure 1: Effect of the object's surface quality on its perceived color

Table 2: Suggested measurement geometries for different coatings

Coating type	Multi-angle	d: 8° by removing the specular component (SCE)	d: 8° by preserving the specular component (SCI)	$45^\circ\text{a}:0^\circ$ Circular annular	$45^\circ\text{a}:0^\circ$ Circular uniplanar	$45^\circ\text{a}:0^\circ$ Single sheet uniplanar
Solid colors (coatings without special effects)	—	*	*	*	*	*

(Continued)

Table 2 (continued)						
Coating type	Multi-angle	d: 8° by removing the specular component (SCE)	d: 8° by preserving the specular component (SCI)	45°a:0° Circular annular	45°a:0° Circular uniplanar	45°a:0° Single sheet uniplanar
Metallic	*	–	*	–	–	–
Shell pigments	*	–	–	–	–	–
Back coating diffusers	*	–	–	–	–	–
Colored aluminum fins	*	–	*	–	–	–
Color changing glass fins	*	–	–	–	–	–
back coating	*	–	*	–	–	–

Note: *Recommended actions.

Table 3: Examining the mirror gloss of a surface

Correct selection of the measuring angle (degrees)	Gloss value at 60 degrees	Gloss range
60	10–70	Medium gloss
20	More than 70	High gloss
85	Less than 10	Low gloss

3 Results and Discussion

3.1 ¹³C-NMR Spectroscopy

The spectra of unmodified lignin and nano-lignin modified diethylenetriamine and propylene carbonate are shown in [Figs. 2 and 3](#). In this test, the number of carbon groups of un-modified lignin and that of modified nano-lignin were calculated based on the peak area. The signals were assigned and the results of the spectrum integration are presented in ([Appendix 1, Table A](#)) the ratio of the integral signal of a certain type of carbon to one-sixth of the integral of the aromatic ring carbons in the spectral range of 0 to 170 ppm and based on [Tables 4 and 5](#).

Comparing the appearance of the spectra in figures and the results of integration ([Appendix 1, Tables B and C](#)) shows that the two samples have significant structural differences. The most important of these differences and their origin is the increase in signal intensity in modified lignin nano-particles compared to un-modified lignin from 6.12 to 6.90 in the range of 160–170 ppm related to phenolic and aliphatic hydroxyl groups.

These small peaks are more noticeable in modified nano-lignin than in un-modified lignin due to the degradation of lignin into smaller nano-particles [[19–22](#)].

Signals at 150–160 ppm are due to the aryl carbon groups that exist in the syringyl ether part of lignin, which has an increasing trend from 7.71 to 13.32 in nano-particles. These peaks are sharper for nano-lignin due to the presence of propylene carbonate and triethylenediamine [[23–26](#)].

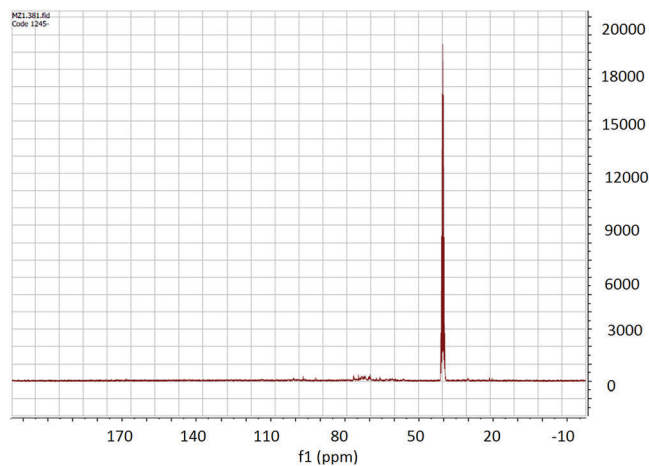


Figure 2: ^{13}C -NMR spectrum obtained from un-modified lignin

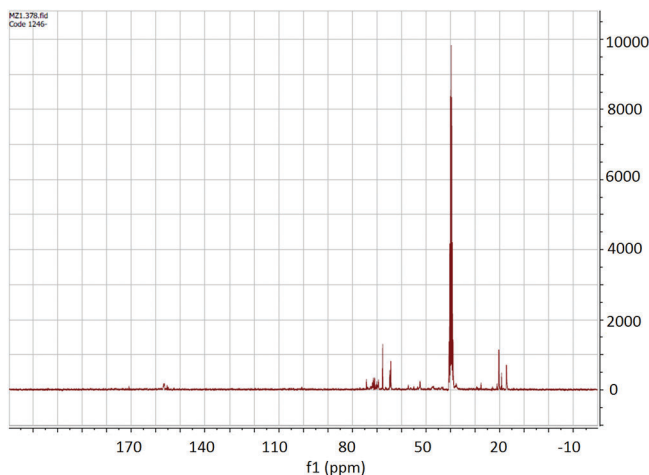


Figure 3: ^{13}C -NMR spectrum obtained from modified nano-lignin

Table 4: Base of ^{13}C -NMR peaks and bonding type of un-modified lignin

Range of peaks (ppm)	Link type
170–175	Phenolic OH
175–160	Aliphatic OH
160–150	C Ar in etherified syringyl units
150–140	C Ar in etherified guaiacyl units
140–130	C Ar in etherified syringyl units
130–110	C Ar in etherified <i>p</i>-coumaric acid ester
110–100	C Ar in syringyl units
70–60	C_α in β-O-4
60–57	C_γ in β-O-4
57–55	CH₃O
55–50	C_β in β-β or β-5

Table 5: Base of ^{13}C -NMR peaks and links type of polyurethane

Range of peaks (ppm)	Link type
20–40	$\text{C}_5\text{H}_9\text{NO}$ (Butyl isocyanate)
12–49	$(\text{CH}_3)_2\text{CO}$ in Triethylamin
11–74	$(\text{CH}_3)_2\text{SO}$
12–38	CH_3CN in Triethylamin
3–4	$\text{C}_4\text{H}_6\text{O}_3$ (propylene carbonate)
3–4	$\text{C}_2\text{H}_3\text{NO}$ (Methyl isocyanate)

The peaks in the area of 100 ppm are related to aryl carbon groups in syringyl, which has a decreasing trend from 10.60 to 8.00. The spectrum shows the facts that both amine and propylene carbonate react with ether groups to form covalent or ionic bonds.

Signals at 55–57 ppm are due to methoxyl groups (CH_3O) directly attached to the benzene ring from lignin fragments during lignin degradation [5,22]. The peaks in this range from 0 to 10.60 have an increasing trend in lignin nano-particles. The increase in signal intensity in modified lignin nano-particles compared to raw lignin from 0 to 10.12 in the range of 50–55 ppm indicates $\text{C}\beta$ in β - β or β -5 bonds of lignin [27].

According to the results, the peaks between 20–40 ppm can represent the isocyanate region related to the CHNO groups resulting from the reaction of amine and carbonate in the lignin modification process. Peaks at 10–12 ppm can represent unreacted amines or CN groups formed as a result of lignin modification with propylene carbonate and triethylenediamine. The results of FTIR obtained from lignin and nano-lignin that were given in previous studies also confirm the results of the ^{13}C -NMR spectrum [4,5].

3.2 Differential Scanning Calorimetric Analysis (DSC)

T_g for lignin, raw lignin, and nano-lignin modified with amine and propylene carbonate based on DSC analysis was observed in the temperature range of 100°C to 120°C. The results show a difference between the flexibility and stiffness of different types of lignin at high temperatures. This information is important in the industrial application of materials.

T_g , molecular weight, and multiple scattering correlations were studied for a series of lignin by Schmidl [28] who observed that the T_g range of the lignin was wide (from 120°C to 170°C), as a result of differences in the pulping methods.

The following Figs. 4–8 show the results of T_g and T_0 values of raw lignin, lignin, and nano-lignin modified with amine EDA, DETA and PC. T_0 was clearly lower in the modified lignin nano-particles compared to the raw and modified lignins. High amounts of modifiers caused more differences in T_g . T_g for different lignin has been reported in the research literature in the range of 90°C to 180°C [29,30].

T_g in lignin nano-particles modified with DETA (112.8°C) and lignin nano-particles modified with EDA (102.5°C) was lower than unmodified lignin (114.6°C) and lignin modified with DETA (126.8°C) and lignin modified with EDA (131.3°C).

It is clearly seen that the effect of lignin modification and the formation of carbonyl groups in it has caused an increase in the crosslink density and an increase in the T_g . The increase of hydroxyl and hydrocarbon groups may be a reason for the increase of the T_g in modified lignins compared to

unmodified lignin and modified nano-lignin. The presence of urethane bonds due to propylene carbonate bonding with amine and C-O bonds may be another reason for this increase.

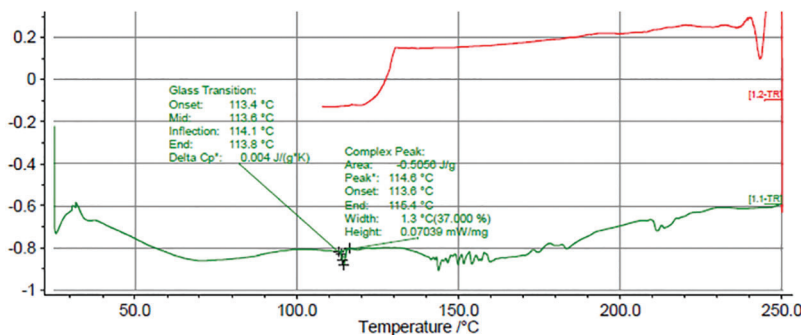


Figure 4: DSC spectrum of mechanical lignin

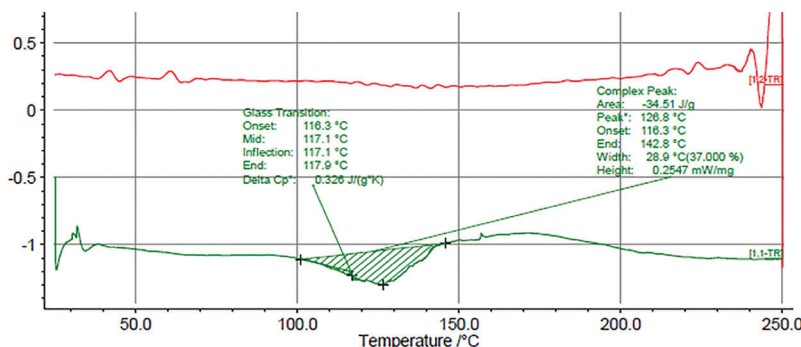


Figure 5: DSC spectrum of lignin modified with DETA

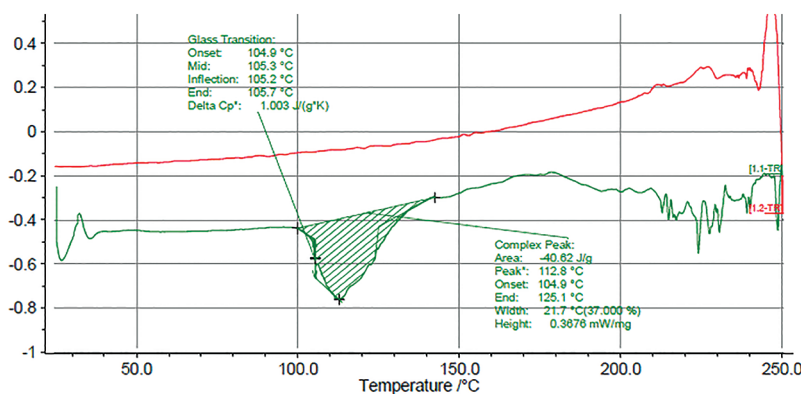


Figure 6: DSC spectrum of nano-lignin modified with DETA

The decrease in the Tg in modified lignin nano-particles compared to un-modified lignin and modified lignin can also be affected by the increase in the cross-sectional area of the particles and the increase in the temperature transfer to the particles and the drop in the Tg.

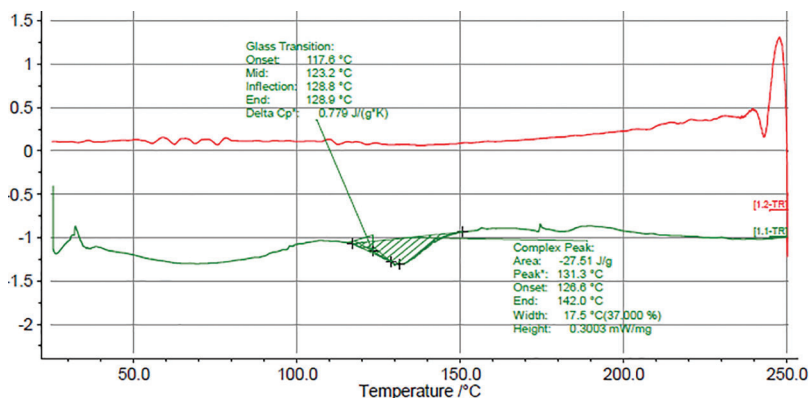


Figure 7: DSC spectrum of lignin modified with EDA

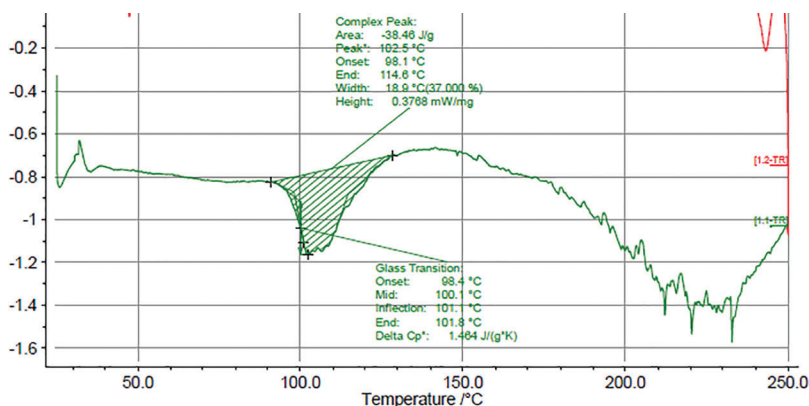


Figure 8: DSC spectrum of nano-lignin modified EDA

It can be concluded that the process of modifying lignin with amine and polypropylene carbonate transforms industrial lignin into a substance that has unique chemical and physical properties. As such, it can be used as a raw material in various applications. For example, lignin with a higher molecular weight and with a lower number of phenolic and acidic hydroxyl groups, can be used as a reinforcement in composite materials. Lignin, which has a lower molecular weight and at the same time more phenolic hydroxyl groups, can be used in bio-softeners or antioxidants. It can be claimed that in PUs, lignin, which has low weight and Tg and high hydroxyl groups, is more desirable. Auto-generated PDF by ReView Green Materials.

3.3 Gel Permeation Chromatography (GPC)

The results of GPC measurements in Figs. 9 and 10 showed that there is a significant difference in the average molecular weight (Mw) and numerical average molecular weight (Mn) values of modified lignin and modified nano-lignin compared to which is reflected in their dispersion index (PDI).

According to the results of Tables 6 and 7, it can be maintained that modified lignin and its soluble and insoluble components have a shorter molecular weight distribution than nano-lignin. Also, in the modified lignin, the average molecular weight and disintegration index are lower than the extracted un-modified lignin. This means that as a result of the process of fractionation and modification of lignin, soluble components with lower molecular weight and fragmentation are obtained compared to the un-modified lignin. Therefore, due to the extraction of this component from unmodified lignin, the remaining

insoluble components have a higher molecular weight and dispersion and a wider molecular weight distribution.

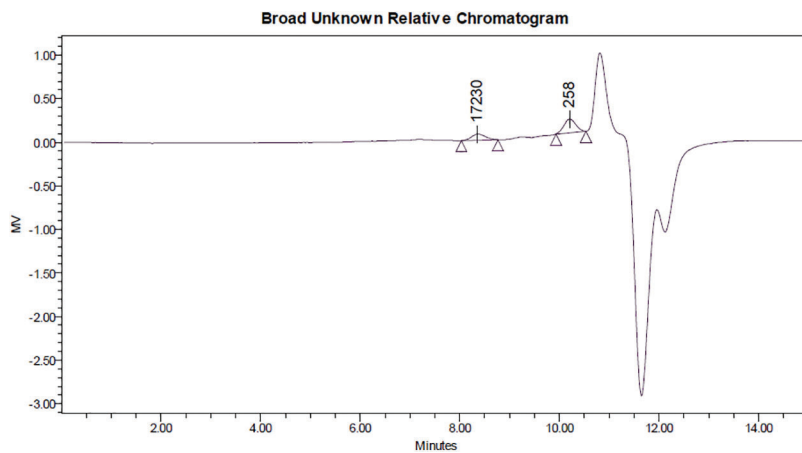


Figure 9: GPC of lignin modified with amine and propylene carbonate

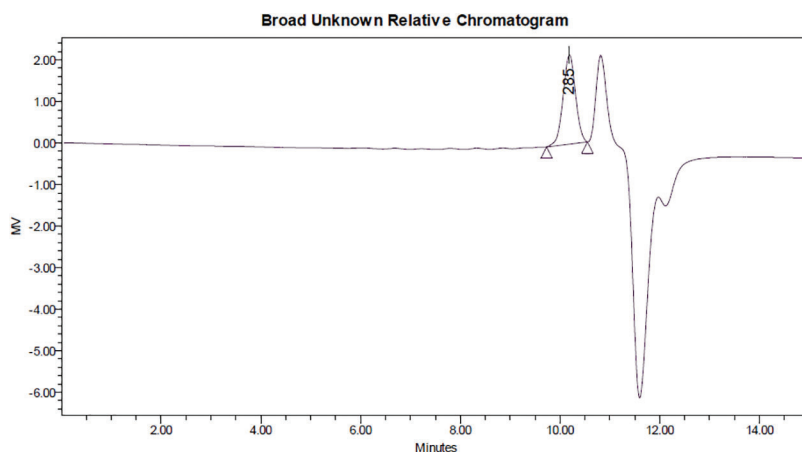


Figure 10: GPC of modified nano-lignin

Table 6: GPC of lignin modified and propylene carbonate and modified nano-lignin

Distribution name	Mn (Daltons)	Mw (Daltons)	MP (Daltons)	Mz (Daltons)	Mz + 1	PDI
Modified nano-lignin	243	265	258	288	312	1.09
Modified lignin	15765	16652	17230	17532	18398	1.05
Modified nano-lignin	275	303	285	376	376	1.101

Table 7: Standard GPC of lignin

Distribution name	Mn (Daltons)	Mw (Daltons)	PDI
Lignin	14149.66	16814.16	1.18

3.4 FE-SEM Electron Microscopy

Fig. 11 shows micrographs of polyurethane coatings based on nano-lignin (7% by weight of petroleum polyol). Contrary to the appearance of the coatings, the nano-particles are not dispersed uniformly on the PU coating. The results also show that the average size of nano-particles in the polyurethane substrate is approximately 500 nm. The largest agglomerates have dimensions of about 2 micrometers. Nano-particles with high surface energy cause a strong tendency to form agglomerates.

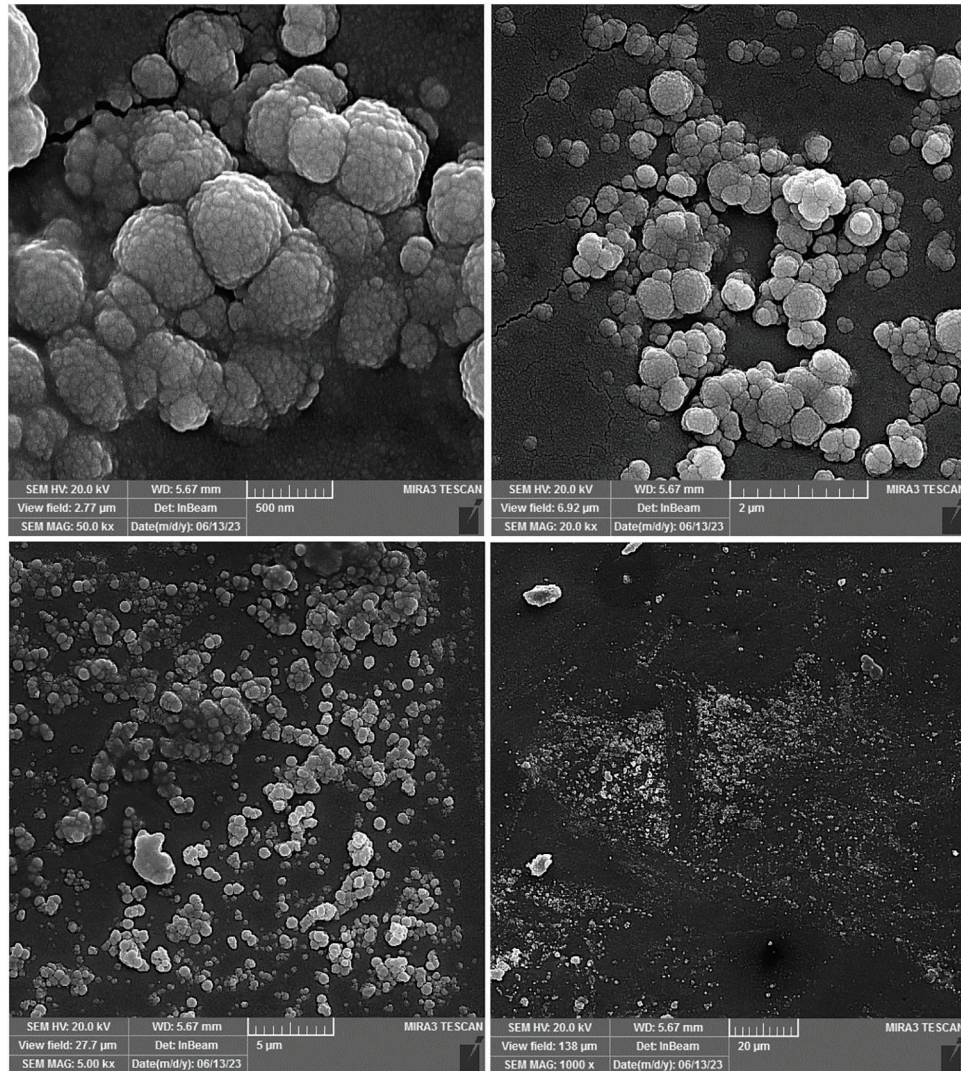


Figure 11: FE-SEM images of the nano-lignin based PU coating

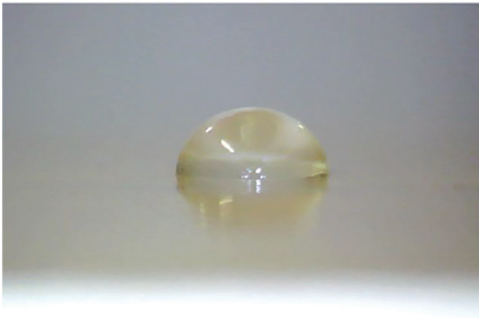
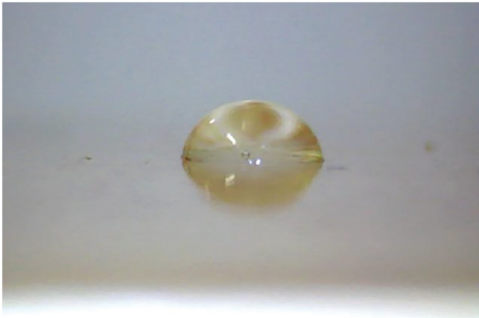
3.5 Surface Roughness and Contact Angle

The surface roughness test showed that the effect of increased content of lignin nano-particles in the coating increased the Ra and Rz values, which is in line with a study by Sow et al. [31].

Table 8 shows the results from the contact-angle measurements. The nano-lignin-based coating has a lower contact angle than the control sample due to the hydrophobic property of nano-lignin particles.

The contact angle change ranges from 0.85° to 0.78° , is too small and can be completely ignored.

Table 8: Contact angle tested on the PU coating after weathering

Row	Sample name	Results (degree)	
1	PU	0.85	
2	DETA	0.78	

3.6 Color Measurements

Table 9 shows the degradation rate of control PU and nano-lignin-based PU coatings before and after the weathering. As can be seen, the amount of redness (a^*) and yellowness (b^*) of the polyurethane coating increased and its whiteness (L^*) decreased after adding lignin nano-particles. After weathering, the color change (ΔE^*) of both coatings was almost the same. However, the change in the amount of yellowness (Δb^*) in the coating containing nano-lignin was significantly lower, which indicates more photoactivity and resistance to the passage of light and more turbidity [32]. The photocatalytic activities of lignin depend on the preparation method, the type of substrate, and the strength of adhesion [33]. PU coating, which contains 7% lignin nano-particles, had a significant advantage over un-modified PU in color change and resistance to moisture and UV rays. Surfaces of lignin nano-particles reduce photoactivity by trapping hydroxyl [34].

Table 9: Color coordinate values and color difference before and after QUV. PU-Polyurethane

Name	Illuminant	Observations	L^*	a^*	b^*	C^*	h^*	ΔL^*	Δa^*	Δb^*	ΔE^*
Nano-lignin PU/Before	D65	10	72.86	7.01	31.81	32.81	77.57				
Nano-lignin PU/After	D65	10	55.35	16.59	36.59	36.34	65.45	-17.51	9.58	4.52	20.47
PU/Before	D65	10	81.40	3.55	23.63	23.90	81.45				
PU/After	D65	10	69.99	10.97	38.11	39.67	73.94	-11.41	7.42	14.48	19.87

The highest degree of surface damage and color change of the coating due to weathering is related to un-modified PU. As the ratio of nano-particles is increased, the amount of surface damage decreases. [Table 9](#) shows that the composite coating is degraded at different rates.

When the number of nano-particles reaches 7% of petroleum polyol, the degradation decreases. The reason for the decrease in the degradation rate of the basic lignin nano-composite coating is the formation of strong lignin bonds with the polyol substrate. It is also possible to mention the phenomenon of photobleaching of lignin coloring groups as another factor. In other words, the decrease in yellowness with the increase in weathering time can be the result of the conversion of paraquinone to hydroquinone groups [35]. [Fig. 12](#) shows the color changes of nano-lignin based Polyurethane before weathering and after weathering.

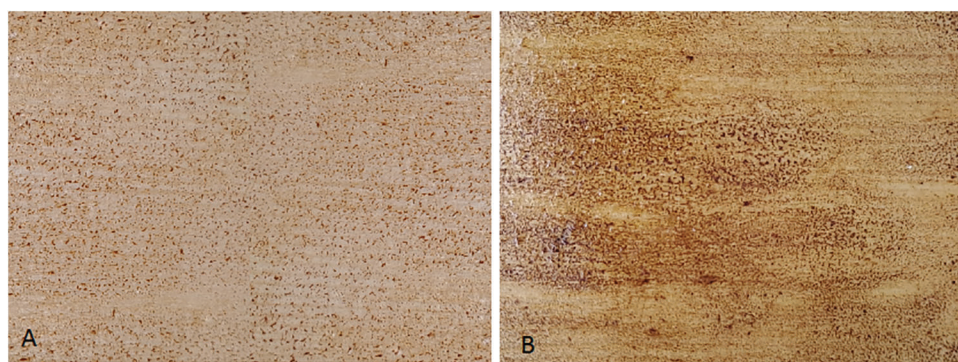


Figure 12: Nano-lignin based polyurethane: A (before weathering), B (after weathering)

3.7 Gloss Test

The gloss-measurement results before and after the accelerated weathering test of PU coating and nano-lignin-based PU coating are shown in [Table 10](#). The un-modified PU coating was more than the nano-particle-based polyurethane coating, which depends on the content of lignin [36]. The reason for gloss reduction in nano-lignin-based polyurethane coating, in addition to particle size and roughness, may be due to its hydroxyl chemical groups. These free groups have a high affinity, which causes the coating to oxidize and further reduce the glossiness of the polyurethane. As can be seen in [Table 11](#), all measured gloss values are in the medium gloss range.

Table 10: Gloss before and after the accelerated weathering test

Gloss value (GU)	Angle		
	85	60	20
PU-Before weathering	59.9	95.1	90.4
PU-After	58.3	93.7	87.6
DETA-Before	60.2	93.6	84.7
DDETA-After	49.6	89.0	80.3

Table 11: Glossiness of one-level rituals

Gloss	Angle of measurement	Gloss range
10 to 70	60°	Medium gloss
70<	20°	High gloss
10>	85°	Low gloss

4 Conclusion

The results of ^{13}C -NMR analyses show that lignin undergoes many structural changes after modification. As observed, the 20–40 ppm peak can represent the urethane and isocyanate region related to the CHNO groups resulting from the reaction of amine and carbonate in the lignin modification process. Also, the FESEM images prepared from the coatings show that the average size of nano-particles in the polyurethane substrate is equal to about 500 nm. The largest agglomerates have dimensions of about 2 micrometers. DSC results also indicate that the glass transition temperature in lignin nano-particles modified with DETA (112.8°C) and lignin nano-particles modified with EDA (102.5°C) is lower than raw lignin (114.6°C) and lignin modified with DETA (126.8°C) and lignin modified with EDA (131.3°C). The results of the color change and gloss test reveal that the surfaces made of lignin nano-particles have more gloss change. Likewise, the results show that lignin nano-particles, by trapping hydroxyl radicals, reduce photoactivity and yellowing activities of nano-lignin-based resin by about 3 times compared to raw polyurethane coatings. Moreover, the results indicate that the nano-lignin-based coating has more roughness and a lower contact angle (0.78 degrees) than the raw polyurethane sample (0.85 degrees).

Acknowledgement: None.

Funding Statement: The authors received specific funding for this study from Tarbiat Modares University of Tehran, Iran.

Author Contributions: The authors declare that all the efforts made for the construction of this work were carried out jointly or in groups, it is not possible to discriminate the role performed by each of the researchers.

Availability of Data and Materials: The data that support the findings of this study are available from the corresponding authors, upon reasonable request.

Conflicts of Interest: The authors declare that they have no conflicts of interest to report regarding the present study.

References

1. Fazeli, A., Ghofrani, M., Hassani Khorshidi, F. (2019). An investigation into the effect of moisture content on adhesion strength of half-polyester and polyurethane clear paints applied to wood surface. *Iranian Journal of Wood and Paper Science Research*, 33(4), 511–521.
2. Hassani Khorshidi, F., Emadi, M. (2017). Studying effect of accelerated aging on adhesion resistance of half polyester and polyurethane transparent coatings applied on maple and pine species. *Iranian Journal of Wood and Paper Science Research*, 32(2), 205–214.
3. Emadi, M., Nazerian, M., Hassani Khorshidi, F. (2022). The effect of magnesium oxide and stone powder additives on the physical properties of wood-cement composite. *Qom Smart Materials Conference*, pp. 1–11. Qom, Iran.
4. Hassani Khorshidi, F., Kazemi Najafi, S., Najafi, F., Pizzi, A., Sandberg, D. et al. (2023). The effect of lignin-based polyols on the properties of polyurethane coatings. In: *Green materials*. <https://doi.org/10.1680/jgrma.23.00040>

5. Hassani Khorshidi, F., Kazemi Najafi, S., Najafi, F., Pizzi, A., Sandberg, D. et al. (2023). The effect of amine type on lignin modification to evaluate its reactivity in polyol construction for non-isocyanate polyurethanes (NIPU). *Journal of Renewable Materials*, 11(5), 2171–2189. <https://doi.org/10.32604/jrm.2023.027835>
6. Lonescu, M. (2005). *Chemistry and technology of polyols for polyurethanes*. 1st ed. UK: Rapra Technology Pub.
7. Adhikari, R., Gunatillake, P. A., Griffiths, I., Tatai, L., Wickramaratna, M. et al. (2008). Biodegradable injectable polyurethanes: Synthesis and evaluation for orthopaedic applications. *Biomaterials*, 29, 3762–3770.
8. Sahnim, W., Boer, F. D., Chapuis, H., Obonou-Akong, F., Pizzi, A. (2022). Feasibility study of the synthesis of isocyanate-free polyurethanes from catechin. *Journal of Renewable Materials*, 10(5), 1175–1184. <https://doi.org/10.32604/jrm.2022.016365>
9. Chen, X., Pizzi, A., Fredon, F. C., Gerardin, C., Zhou, X. (2022). Low curing temperature tannin-based non-isocyanate polyurethane (NIPU) wood adhesives: Preparation and properties evaluation. *International Journal of Adhesion and Adhesives*, 112, 103001. <https://doi.org/10.1016/j.ijadhadh.2021.103001>
10. Azadeh, E., Chen, X., Pizzi, A., Gerardin, C., Gerardin, P. (2022). Self-blowing non-isocyanate polyurethane foams based on hydrolysable tannins. *Journal of Renewable Materials*, 10(12), 3217–3227. <https://doi.org/10.32604/jrm.2022.022740>
11. Cornille, A., Blain, M., Auvergne, R., Andrioletti, B., Boutevin, B. et al. (2017). A study of cyclic carbonate aminolysis at room temperature: Effect of cyclic carbonate structures and solvents on polyhydroxyurethane synthesis. *RSC Polymer Chemistry*, 8, 592–604.
12. Quienne, B., Poli, R., Pinaud, J., Caillol, J. (2021). Enhanced aminolysis of cyclic carbonates by β -hydroxylamines for the production of fully biobased polyhydroxyurethanes. *RSC Green Chemistry*, 23, 1678–1690.
13. Ecochard, Y., Caillol, S. (2020). Hybrid polyhydroxyurethanes: How to overcome limitations and reach cutting edge properties. *Polymer*, 137, 109915.
14. Tim, R., Cooper, F., Robson, F. (2008). Poly(lactic acid) and chain-extended poly(lactic acid)-polyurethane functionalized with pendent carboxylic acid groups. *Macromolecules*, 41, 655–662.
15. Zeng, J., Li, Y., Zhu, Q., Yang, K., Wang, X. et al. (2009). A novel biodegradable multiblock poly(ester urethane) containing poly(L-lactic acid) and poly(butylene succinate) blocks. *Polymer*, 50, 1178–1186.
16. ASTM (American Society for Testing and Materials) (2022). ASTM D4273-23. Standard test method for polyurethane raw materials: Determination of primary hydroxyl content of polyether polyols. ASTM International, West Conshohocken, Pennsylvania, USA.
17. ASTM (American Society for Testing and Materials) (2014). ASTM E1356-08. Standard test method for assignment of the glass transition temperatures by differential scanning calorimetry. ASTM International, West Conshohocken, Pennsylvania, USA.
18. ASTM (American Society for Testing and Materials) (2019). ASTM D4587-11. Standard practice for fluorescent UVCondensation exposures of paint and related coatings. ASTM International, West Conshohocken, Pennsylvania, USA.
19. Saražin, J., Pizzi, A., Amirou, S., Schmiedl, D., Šernek, M. (2021). Organosolv lignin for non-isocyanate based polyurethanes (NIPU) as wood adhesive. *Journal of Renewable Materials*, 9(5), 881–907. <https://doi.org/10.32604/jrm.2021.015047>
20. Xi, X., Pizzi, A., Delmotte, L. (2018). Isocyanate-free polyurethane coatings and adhesives from mono- and di-saccharides. *Polymers*, 10, 402.
21. Xi, X., Wu, Z., Pizzi, A., Gerardin, C., Lei, H. (2019). Non-isocyanate polyurethane adhesive from sucrose used for particleboard. *Wood Science and Technology*, 53(2), 393–405.
22. Xi, X., Pizzi, A., Gerardin, C., Lei, H., Chen, X. (2019). Preparation and evaluation of glucose based non-isocyanate polyurethane selfblowing rigid foams. *Polymers*, 11, 1802.
23. Chen, X., Li, J., Xi, X., Pizzi, A., Zhou, X. (2020). Condensed tannin-glucose-based NIPU bio-foams of improved fire retardancy. *Polymer Degradation and Stability*, 175, 109121.
24. Beneš, H., Paruzel, A., Hodan, J., Trhlíková, O. (2018). Impact of natural oil-based recycled polyols on properties of cast polyurethanes. *Journal of Renewable Materials*, 6(7), 697–706. <https://doi.org/10.32604/JRM.2018.00011>

25. Chen, X., Xi, X., Pizzi, A., Fredon, E., Zhou, X. (2020). Preparation and characterization of condensed tannin non-isocyanate polyurethane (NIPU) rigid foams by ambient temperature blowing. *Polymers*, 12, 750.
26. Chen, X., Pizzi, A., Xi, X., Zhou, X., Fredon, F. (2021). Soy protein isolate non-isocyanates polyurethanes (NIPU) wood adhesives. *Journal of Renewable Materials*, 9(6), 1045–1057. <https://doi.org/10.32604/jrm.2021.015066>
27. Baumberger, S., Abaecherli, A., Fasching, M., Gellerstedt, G., Gosselink, R. (2007). Molar mass determination of lignins by size exclusion chromatography: Towards standardisation of the method. *Holzforschung*, 61(4), 459–468.
28. Schmidl, G. (1992). *Molecular weight characterization and rheology of lignins for carbon fibers (Ph.D. Thesis)*. University of Florida, Gainesville, FL, USA.
29. Jain Rajesh, K., Glasser Wolfgang, G. (1993). Lignin derivatives. II. Functional ethers. *Holzforschung*, 47(4), 325–332.
30. Tejado, A., Peña, C., Labidi, J., Echeverria, J. M., Mondragon, I. (2007). Physico-chemical characterization of lignins from different sources for use in phenol-formaldehyde resin synthesis. *Bioresource Technology*, 98(8), 1655–1663.
31. Sow, C., Riedl, B., Blanchet, P. (2010). UV-waterborne polyurethane-acrylate nano-composite coatings containing alumina and silica nano-particles for wood: Mechanical, optical, and thermal properties assessment. *Journal of Coatings Technology and Research*, 8(2), 211–221.
32. Luo, Z., Cai, H., Liu, J., Hong, W., Tang, S. (2005). Preparation of TiO₂ on the glass and hydrophilicity under sunlight irradiation. *Key Engineering Materials*, 283, 827–830.
33. Jang, S. H., Kim, D. H., Park, D. H., Kim, O. Y., Hwang, S. H. (2018). Construction of sustainable polyurethane-based gel-coats containing poly(ϵ -caprolactone)-grafted lignin and their coating performance. *Progress in Organic Coatings*, 120, 234–239.
34. Bunhu, T., Kindness, A., Martincigh, B. (2011). Determination of titanium dioxide in commercial sunscreens by inductively coupled plasma-optical emission spectrometry. *Renewable Energy*, 64, 139–143.
35. Darabi, L. (2010). Investigating the effect of methylation and antioxidant on the color change of weathered wood plastic composites. *Iranian Journal of Wood and Paper Industries*, 1(1), 12–26.
36. Safi, M., Khalili, N. (2019). Effect of measurement geometry on colorimetry of glossy white samples. *Color Science and Technology*, 14(3), 237–246.

Appendix 1

Table A: ^{13}C -NMR peaks of un-modified lignin

Peak (ppm)	Intensity	Range of peaks (ppm)	Total intensity
172.1040	6.129396e-001	175–160	6.129396e-001
102.2379	7.717050e-001	100–90	7.717050e-001
98.1450	1.294400e+000	90–80	10.623932e-001
92.9124	9.329532e-001		
77.1056	1.464874e+000	80–70	29.487161e-001
75.1287	1.800253e+000		
74.4727	9.439274e-001		
74.2988	8.551857e-001		
73.5634	1.354750e+000		
73.0844	1.063059e+000		
72.6951	1.302872e+000		
72.3101	1.449842e+000		
70.9901	1.221045e+000		
70.5558	1.214769e+000		
70.2039	1.845611e+000		
67.6385	8.687168e-001	70–60	15.64837e+000
66.0913	1.088551e+000		
61.9919	5.872651e-001		
60.8856	6.363314e-001	60–50	6.363314e-001
40.6895	1.500000e+001	50–40	15.044933e+001
40.4118	4.532829e+001		
40.1342	9.012104e+001		
39.8567	1.056048e+002	40–30	15.998145
39.5790	8.970615e+001		
39.3015	4.491465e+001		
39.0239	1.480017e+001		
29.4370	8.676242e-001	30–20	8.676242e-001
20.4260	8.843964e-001	20–10	17.543506e-001
19.3149	8.699542e-001		

Table B: ^{13}C -NMR peaks of modified nano-lignin

Peak pick details (ppm)	Intensity	Range of peaks (ppm)	Total intensity
170.9336	9.676529e-001	170–160	9.676529e-001
156.7831	1.860762e+000	160–150	13.327222e+000
156.5143	1.888217e+000		
155.4147	1.248927e+000		
154.8872	8.329328e-001		
100.5658	8.004947e-001	100–80	8.004947e-001
74.2730	3.225467e+000	80–70	43.060158e+000
73.8610	7.791835e-001		
72.6600	1.009155e+000		
72.3462	9.877460e-001		
71.8599	2.163699e+000		
71.4499	3.614719e+000		
70.9699	3.700205e+000		
70.3949	1.511643e+000		
70.1452	2.517968e+000		
70.0320	7.648007e-001		
69.7507	1.469372e+000	70–60	28.796069e+000
69.4511	3.100555e+000		
67.6688	1.439026e+001		
66.4831	7.919319e-001		
64.824	5.984829e+000		
64.3675	8.882968e+000		
57.2739	1.423347e+000	60–50	21.9529e+000
54.9925	9.289600e-001		
53.4445	8.616349e-001		
52.4544	2.623604e+000		
46.9362	1.021684e+000	50–40	32.537445e+000
43.6040	7.966582e-001		
43.0888	8.331347e-001		
40.6606	1.500000e+001		
40.3837	4.558033e+001		
40.1059	9.159799e+001		
39.8283	1.075290e+002	40–30	18.2800779e+000
39.5508	9.123924e+001		
39.2729	4.595969e+001		

(Continued)

Table B (continued)			
Peak pick details (ppm)	Intensity	Range of peaks (ppm)	Total intensity
38.9962	1.553697e+001		
37.7648	1.931570e+000		
29.4373	8.770423e-001	30–20	28.850416e+000
27.6544	2.083079e+000		
22.9989	8.587693e-001		
21.1090	1.809882e+000		
20.4188	6.361032e+000		
20.3683	1.238307e+001		
19.5619	9.288253e-001	20–10	26.268494e+000
19.3125	5.086354e+000		
19.2808	4.218895e+000		
17.3201	7.674992e+000		

Table C: ¹³C-NMR comparison of un-modified lignin and modified nano-lignin

Range of peaks (ppm)	Total intensity of nano modified lignin	Total intensity of lignin
170–160	9.676529e-001	6.129396e-001
160–150	13.327222e+000	7.717050e-001
100–80	8.004947e-001	10.623932e-001
80–70	43.060158e+000	29.487161e-001
70–60	28.796069e+000	15.64837e+000
60–50	21.9529e+000	6.363314e-001
50–40	32.537445e+000	15.044933e+001
40–30	18.2800779e+000	15.998145
30–20	28.850416e+000	8.676242e-001
20–10	26.268494e+000	17.543506e-001